Applications and Applied Mathematics: An International Journal (AAM)

Volume 18 | Issue 1 | Article 20

6-2023

(R2033) Resonant Curve Due to Perturbations of Geo-Synchronous Satellite including Effect of Earth's Equatorial Ellipticity

Sushil Yadav
University of Delhi

Mukesh Kumar
University of Delhi

Virendra Kumar
University of Delhi

Available at
http://pvamu.edu/aam
Appl. Appl. Math.
ISSN: 1932-9466

Applications and Applied Mathematics:
An International Journal
(AAM)

Vol. 18, Issue 1 (June 2023), Article 20, 14 pages

Resonant Curve Due to Perturbations of Geo-Synchronous Satellite Including Effect of Earth's Equatorial Ellipticity

[1]Sushil Yadav, [2*]Mukesh Kumar and [3]Virendra Kumar

[1]Department of Mathematics
Maharaja Agrasen College
University of Delhi
Delhi, India
syadav@mac.du.ac.in

[2*]Department of Mathematics
Shyam Lal College
University of Delhi
Delhi, India
mukesh@shivaji.du.ac.in

[3]Department of Mathematics
Dualat Ram College
University of Delhi
Delhi, India
[3]vmath.du@gmail.com

*Corresponding Author

Received: October 26, 2022; Accepted: May 5, 2023

Abstract

In this paper, we have investigated resonant curve due to frequencies − angular rate of rotation of the Earth and the rate of change of Earth's equatorial ellipticity parameter. Perturbation equations are used to convert the non-linear equations of motion of geo-synchronous satellite to the linear form. With the help of graphs, we have shown the effect of Earth's equatorial ellipticity parameter on oscillatory amplitude and variation in orbital radius of satellite. By defining different perturbations, we have also drawn resonant curve due to frequencies steady-state orbital angular rate of satellite and the rate of change of Earth's equatorial ellipticity parameter. we have analyzed the undamped and unforced phase portrait and phase space by using the method of Poincare section. Finally, we have obtained energy integral and motion of the mean longitude for the geo-synchronous satellite in the set of axis rotating with Earth.

Keywords: Earth's equatorial ellipticity; Geo-synchronous satellite; Perturbations; Resonance

MSC 2010 No.: 37N05, 70F07, 70F15, 34F15

1. Introduction

In recent years, geo-synchronous satellite orbit resonant with respect to perturbing influence of the gravitational field of Earth has been studied widely. There are many forces which affect the motion of the geo-synchronous satellite like Earth's gravitational force, solar radiation pressure, relativistic effect, etc.

When two satellites or planets repeat their geometric configuration with respect to their orbits within a period of time, then we say that resonance occurs. In the circular and elliptical case, the resonance was studied by Bhatnagar and Gupta (1977) in the restricted three-body problem. They have also studied resonance in two rigid spheroids and in the artificial Earth's satellite. Garfinkel (1982) studied the resonance problem in the celestial mechanics. He formulated the method and found the solution for the resonance problem. Stevan and Holmes (1983) studied the phase portrait and Poincare section by considering non-linear oscillator with single degree of freedom and non-linear restoring force. Bhatnagar and Kaur (1990) studied the in-plane motion of geo-synchronous satellite caused by the attraction of the Sun, the Moon and the Earth including oblateness and Earth's equatorial ellipticity parameter. Breiter (1999) investigated a family of resonance, unstable and stable points. He also studied the luni-solar resonance problem. Radwan (2002) studied the resonance between the motion of the satellite, the Sun and the Moon by taking oblateness of the Earth and Luni-solar attraction. Formiga and de Moraes (2011) studied the motion of the satellite and resonance between two frequencies of the Earth rotational motion and mean orbital motion by using geopotential perturbations.

In previous related work, Yadav and Aggarwal (2013) have studied the effect of Earth's equatorial ellipticity on the amplitude and time period of the resonant oscillations but they ignored the study of resonant curve due to the commensurability between the frequencies $\dot{\theta}_E$ (angular rate of rotation of the Earth) and $\dot{\gamma}$ (rate of change of Earth's equatorial ellipticity parameter).

Equations of motion in our study are in agreement with the equations of motion of Frick and Garber (1962) if $J_2^{(2)}$ terms are neglected. The phase portrait is drawn in our study for the undamped and unforced system is similar to the phase portrait drawn by Stevan and Holmes (1983) in the non-linear oscillatory system for undamped and unforced system.

The present study of geo-synchronous satellite with resonance has many applications in telecommunication as they are directly over the equator and visible from the large area of Earth's surface. Geo-synchronous satellites are also used in meteorological department for weather forcasting, remote sensing, oceanography, stationkeeping on a spacecraft in the vicinity of Libration points orbit as part of trajectory design in the Earth-Moon system and atmospheric tracing. Also, it is used in navigation purposes.

Kaur et al. (2018) studied the resonance problems of geo-centric satellite due to Poynting-Robertson Drag. They assumed that the Sun, the Earth and the satellite lies in the same plane and found resonance points between the angular velocity of Earth and mean motion of satellite. Yadav et al. (2019) investigated the location and stability of Lagrangian points in the problem of geo-centric satellite including Earth's equatorial ellipticity. They observed that for different values for Γ, the Lagrangian points exist infinitely. Cai et al. (2020) analyzed the chlorophyll-a distribution in the Sea area from the geo-synchronous satellite. Hashimoto et al. (2021) studied the Amazon canopy using Advanced Baseline Imager of new generation of geo-stationary satellite.

This paper is organized as follows. In Section 2, we have expressed equations of motion of geo-synchronous satellite using Earth's gravitational potential by following the procedure of Frick and Garber (1962). In Section 3, we defined the perturbations relative to the synchronous orbit and also found the solution. We have drawn resonant curve and shown the effect of γ on Δr in Section 4. In Section 5, we have shown the phase portrait for the undamped and unforced oscillations. We have also described the phase space with the help of Poincare section. In Section 6, we have obtained the energy integral in the set of axis rotating with Earth. We have also found equilibrium points and motion of the mean longitude. In Section 7, we discussed and analysed the results.

2. Equations of Motion

We have taken xyz system as inertial reference with origin at the Earth's center and Oz be the polar axis. The position of satellite P is in the spherical coordinates θ, ϕ and r. OA is the instantaneous position of the minor axis of the Earth's equatorial section (Figure 1).

Let angle γ be the measured from minor axis of the Earth's equatorial ellipse to the projection of the satellite (Figure 2).

We take the Earth's gravitational potential and following the procedure of Frick and Garber (1962) to find force components.

Therefore, equations of motion of the satellite in spherical polar coordinate $P(r, \theta, \phi)$ can be written as

$$\ddot{r} - r\dot{\theta}^2\cos^2\phi - r\dot{\phi}^2 = -\frac{g_0R_0^2}{r^2} + \frac{3J_2g_0R_0^4}{r^4}\left(\frac{3\sin^2\phi - 1}{2}\right) - \frac{9J_2^{(2)}g_0R_0^4\cos^2\phi\cos 2\gamma}{r^4},$$

$$\frac{1}{r\cos\phi}\frac{d}{dt}(r^2\dot{\theta}\cos^2\phi) = -\frac{6J_2^{(2)}g_0R_0^4\cos\phi\sin 2\gamma}{r^4},$$

$$\frac{1}{r}\frac{d}{dt}(r^2\dot{\phi}) + r\dot{\theta}^2\cos\phi\sin\phi = -\frac{3J_2g_0R_0^4\cos\phi\sin\phi}{r^4} - \frac{6J_2^{(2)}g_0R_0^4\cos\phi\sin\phi\cos 2\gamma}{r^4},$$

where

$r =$ radial distance of the satellite from the center of the Earth,

$R_0 = 6.3781 \times 10^6$ m $=$ radius of the Earth,

$g_0 = 9.8$ m/s^2 $=$ gravitational acceleration at the Earth's surface,

$J_2 = 1.08219 \times 10^{-3}$ $=$ Earth oblateness coefficient,

$J_2^{(2)} = -5.35 \times 10^{-6}$ $=$ equatorial ellipticity coefficient,

$\gamma = \theta - \theta_E$ (Figure 1).

This can be simplified as (assuming ϕ to be very small)

$$\ddot{r} - r\dot{\theta}^2 = -\frac{g_0 R_0^2}{r^2} - \frac{3J_2 g_0 R_0^4}{2r^4} - \frac{9J_2^{(2)} g_0 R_0^4 \cos 2\gamma}{r^4}, \tag{1}$$

$$\frac{1}{r}\frac{d}{dt}(r^2\dot{\theta}) = -\frac{6J_2^{(2)} g_0 R_0^4 \sin 2\gamma}{r^4}. \tag{2}$$

3. Perturbations Relative to Synchronous Orbit

We define

$$r = r_c + \Delta r,$$
$$\theta = \theta_E + \gamma_0 + \Delta\gamma,$$

where r_c is the orbital radius of a synchronous orbit $(r_c = 42164\,\text{Km})$ and γ_0 is longitude difference between minor axis of the Earth's equatorial and the position the synchronous satellite.

In the above perturbation equations, r_c is very large in comparison to Δr. So, $\frac{\Delta r}{r_c}$, being very small, may be neglected.

Equations (1) and (2) can be written as

$$\Delta\ddot{r} - \dot{\theta}_E^2 \Delta r = r_c\dot{\theta}_E^2 + 2r_c\dot{\theta}_E\Delta\dot{\gamma} - \frac{g_0 R_0^2}{r_c^2} - \frac{3J_2 g_0 R_0^4}{2r_c^4} - \frac{9J_2^{(2)} g_0 R_0^4}{r_c^4}\cos 2\gamma\,, \tag{3}$$

and

$$\frac{d}{dt}(r_c^2\Delta\dot{\gamma} + 2r_c\dot{\theta}_E\Delta r) = -\frac{6J_2^{(2)} g_0 R_0^4}{r_c^3}\sin 2\dot{\gamma}t. \tag{4}$$

On integrating Equation (4), we get

$$r_c^2\Delta\dot{\gamma} + 2r_c\dot{\theta}_E\Delta r = \frac{3J_2^{(2)} g_0 R_0^4}{\dot{\gamma}\; r_c^3}\cos 2\gamma + c, \tag{5}$$

where c is constant of integration to be determined by using initial condition when $t = t_0$ then $\Delta r = \Delta r_0$ $\Delta\dot{\gamma} = 0$. So, we get

$$c = 2r_c\dot{\theta}_E\Delta r_0 - \frac{3J_2^{(2)} g_0 R_0^4}{\dot{\gamma}\; r_c^3}\cos 2\dot{\gamma}t_0.$$

Substituting above value of c in Equation (5), we get

$$r_c\Delta\dot{\gamma} = -2\dot{\theta}_E(\Delta r - \Delta r_0) + \frac{3J_2^{(2)} g_0 R_0^4}{\dot{\gamma}\; r_c^4}\cos 2\dot{\gamma}t - \frac{3J_2^{(2)} g_0 R_0^4}{\dot{\gamma}\; r_c^4}\cos 2\dot{\gamma}t_0. \tag{6}$$

Substituting the value of $r_c \Delta\dot{\gamma}$ from Equation (6) in Equation (3), we get

$$\Delta\ddot{r} + 3\dot{\theta}_E^2 \Delta r = 4\dot{\theta}_E^2 \Delta r_0 + r_c \dot{\theta}_E^2 - \frac{g_0 R_0^2}{r_c^2} - \frac{3J_2 g_0 R_0^4}{2r_c^4} + K\cos 2\dot{\gamma}t - \frac{6\dot{\theta}_E J_2^{(2)} g_0 R_0^4}{\dot{\gamma}\, r_c^4} \cos 2\dot{\gamma}t_0 \ , \tag{7}$$

where

$$K = \frac{3J_2^{(2)} g_0 R_0^4}{r_c^4} \left(2\frac{\dot{\theta}_E}{\dot{\gamma}} - 3 \right).$$

Since our aim is to study resonance due to frequencies $\dot{\theta}_E$ and $\dot{\gamma}$, we ignore secular terms. We get

$$\Delta\ddot{r} + 3\dot{\theta}_E^2 \Delta r = K\cos 2\dot{\gamma}t, \tag{8}$$

which is non-homogeneous second order differential equation.

A particular solution of Equation (8) is

$$\Delta r = A\cos 2\dot{\gamma}t,$$

where

$$A = \frac{K}{3\dot{\theta}_E^2 - 4\dot{\gamma}^2}.$$

4. Resonance at the Point Where $3\dot{\theta}_E^2 = 4\dot{\gamma}^2$

We have drawn graphs using dimensionless coordinates by assuming that orbital radius of satellite ($r_c = 42164$ Km), mass of Earth (5.972×10^{24} Kg) and universal gravitational constant (G) as 1 unit, i.e., 1 m $= 2.3716949 \times 10^{-8}$ units, 1 Kg $= 0.167248091 \times 10^{-24}$ units, 1 Sec $= 473620$ units.

From the expression of oscillatory amplitude A, it is found that A becomes indeterminate if $\frac{\dot{\gamma}^2}{\dot{\theta}_E^2} = \frac{3}{4}$.

So, resonance occurs at the point where $\frac{\dot{\gamma}^2}{\dot{\theta}_E^2} = \frac{3}{4}$.

From Figure 3, we observed that the amplitude A becomes indeterminate (resonance occurs) at $\frac{\dot{\gamma}^2}{\dot{\theta}_E^2} = \frac{3}{4}$.

In Figure 4, we observed that Δr increases with respect to time t.

In Figure 5, oscillatory amplitudes are changing when values of γ increases. There is small effect of Earth's equatorial ellipticity parameter on oscillatory amplitude.

In Figure 6, we have shown the point R where resonance occurs and amplitude becomes indeterminate in three-dimensional graph.

Similarly, by defining the following different perturbations relative to synchronous orbit

$$r = r_c + \Delta r,$$
$$\theta = \theta_0 + \gamma_0 + \Delta\theta,$$

where θ_0 is steady-state value of θ and following the same procedure, we obtain

$$\Delta\ddot{r} + 3\dot{\theta}_0^2 \Delta r = K \cos 2\dot{\gamma}t, \tag{9}$$

where $\dot{\theta}_0$ is steady-state orbital angular rate of geo-synchronous satellite.

A particular solution of Equation (9) is

$$\Delta r = A \cos 2\dot{\gamma}t,$$

where

$$A = \frac{K}{3\dot{\theta}_0^2 - 4\dot{\gamma}^2}.$$

Here, amplitude A becomes inderminate when $3\dot{\theta}_0^2 = 4\dot{\gamma}^2$, i.e., resonance occur between the frequencies $\dot{\theta}_0$ and $\dot{\gamma}$.

Now, it can be observed that resonant curve due to the frquencies $\dot{\theta}_0$ and $\dot{\gamma}$ is similar to the Figure 3.

In Figure 7, we observed that Δr increases when time t increases.

In Figure 8, oscillatory amplitudes are changing when values of γ increases. There is small effect of Earth's equatorial ellipticity parameter on oscillatory amplitude.

In Figure 9, we have shown the point R where resonance occurs and amplitude becomes indeterminate in three-dimensional graph.

5. Phase Portrait and Poincare Section

5.1. Phase Portrait

Phase portrait is a continuous family of closed orbits. Phase potrait of the differential equation $\Delta\dot{s} = -3\dot{\theta}_E^2 \Delta r$ ($\Delta s = \Delta\dot{r}$) is parametric curves on the plane which trace the path of the particular solution. This plane is called phase plane. The undamped, unforced phase plane for the Equation (8) is shown in Figure 10.

5.2. Poincare Section

We can study Equation (8) by applying the method of Poincare section. The periodically forced oscillations has 3-dimentional extended phase space with coordinates $(t, \Delta r, \Delta s)$ (where $\Delta s =$

$\Delta\dot{r}$). It is observed that vector field Equation (8) is periodic in t with period $\frac{\pi}{\dot{\gamma}}$. Orbits in the phase space $(t, \Delta r, \Delta s)$ are described by the mapping $P : \sum \to \sum$ induced by the solution

$$\Delta r = A\cos(\sqrt{3}\dot{\theta}_E(t-t_0)) + B\sin(\sqrt{3}\dot{\theta}_E(t-t_0)) + \frac{K}{3\dot{\theta}_0^2 - 4\dot{\gamma}^2}\cos 2\dot{\gamma}t, \tag{10}$$

where $\sum = \{(t, \Delta r, \Delta s) | \Delta r = 0, \Delta s > 0\}$, is Poincare section. Figure 11 describes the phase space $(t, \Delta r, \Delta s)$ showing Poincare section $\sum$ with periodicty $\frac{\pi}{\dot{\gamma}}$ in t. It is also observed that the flow of differential equation

$$\Delta\dot{r} = \Delta s, \qquad \Delta\dot{s} = K\cos(2\dot{\gamma}t) \tag{11}$$

for $\Delta s > 0$, $\Delta\dot{r} \neq 0$ is everywhere transverse to $\sum$.

6. Energy Integral in the Set of Axis Rotating with Earth

The energy integral E per unit mass is given by

$$E = \frac{v^2}{2} - U - \frac{\dot{\theta}_E^2\, r^2\cos^2\phi}{2}, \tag{12}$$

where

$$v^2 = \dot{r}^2 + r^2\dot{\theta}^2\cos^2\phi + r^2\dot{\phi}^2,$$

and

$$U = \frac{g_0 R_0^2}{r}\Big[1 - J_2\frac{R_0^2}{r^2}\left(\frac{3\sin^2\phi - 1}{2}\right) + 3\frac{J_2^{(2)} R_0^2}{r^2}\cos^2\phi\cos 2\gamma\Big].$$

By substituting the values of U (Frick and Garber (1962)) and v in Equation (12) and after simplification, we get

$$\begin{aligned} E =& \frac{\dot{r}^2}{2} + \frac{r^2\dot{\theta}^2\cos^2\phi}{2} + \frac{r^2\dot{\phi}^2}{2} - \frac{g_0 R_0^2}{r}\Big[1 - J_2\frac{R_0^2}{r^2}\left(\frac{3\sin^2\phi - 1}{2}\right) + 3\frac{J_2^{(2)} R_0^2}{r^2}\cos^2\phi\cos 2\gamma\Big] \\ & - \frac{\dot{\theta}_E^2\, r^2\cos^2\phi}{2}. \end{aligned} \tag{13}$$

The equilibrium points of the sum

$$U + \frac{\dot{\theta}_E^2\, r^2\cos^2\phi}{2} = f(r,\theta,\phi) \text{ (supposed)}, \tag{14}$$

are the minimum and saddle points of the function f. These points may be obtained by solving the following three equations.

$$\frac{\partial f}{\partial r} = 0$$

$$\implies \Big[-\frac{g_0 R_0^2}{r^2} + \frac{3J_2 g_0 R_0^4\left(3\sin^2\phi - 1\right)}{2\,r^4} - \frac{9J_2^{(2)} g_0 R_0^4\cos^2\phi\cos 2\gamma}{r^4}\Big] + \dot{\theta}_E^2\, r\cos^2\phi = 0, \tag{15}$$

$$\frac{\partial f}{\partial \theta} = 0$$

$$\implies \left[-\frac{6J_2^{(2)} g_0 R_0^4 \cos^2\phi \sin 2\gamma}{r^3}\right] = 0, \tag{16}$$

and

$$\frac{\partial f}{\partial \phi} = 0$$

$$\implies \Big[-\frac{3J_2 g_0 R_0^4 \cos\phi \sin\phi}{r^3} - \frac{6J_2^{(2)} g_0 R_0^4 \cos\phi \sin\phi \cos 2\gamma}{r^3}\Big] + \dot{\theta}_E^2 \ r \cos\phi \sin\phi = 0. \tag{17}$$

The motion of the mean longitude L near synchronous satellite is given by

$$\frac{R^2}{2}\left(\frac{dL}{dt}\right)^2 + 3\left[U + \frac{\dot{\theta}_E^2 \ r^2 \cos^2\phi}{2}\right] = 0, \tag{18}$$

where $R = 42164$ Km.

By substituting the value of U and after simplification, we get

$$L = \Big(\frac{6}{R^2}\Big[\frac{J_2 \ g_0 \ R_0^4}{r^3}\left(\frac{3\sin^2\phi - 1}{2}\right) - \frac{g_0 R_0^2}{r} - \frac{3 \ J_2^{(2)} \ g_0 \ R_0^4 \cos^2\phi \cos 2\gamma}{r^3} - \frac{\dot{\theta}_E^2 \ r^2 \cos^2\phi}{2}\Big]\Big)^{\frac{1}{2}} t + C,$$

where C be an integral constant, at $t = 0$, $L = 0$, we have $C = 0$;

then,

$$L = \Big(\frac{6}{R^2}\Big[\frac{J_2 \ g_0 \ R_0^4}{r_c^3}\left(\frac{3\sin^2\phi - 1}{2}\right) - \frac{g_0 R_0^2}{r_c} - \frac{3 \ J_2^{(2)} \ g_0 \ R_0^4 \cos^2\phi \cos 2\gamma}{r_c^3} - \frac{\dot{\theta}_E^2 \ r_c^2 \cos^2\phi}{2}\Big]\Big)^{\frac{1}{2}} t. \tag{19}$$

7. Conclusions

We used perturbation technique to convert non-linear equations of motion of geo-synchronous satellite to linear form. Then, we obtained a second order linear differential equation and from the particular solution of that equation, we found that resonance occurs due to frequencies− angular rate of rotation of the Earth and the rate of change of Earth's equatorial ellipticity parameter. We have also drawn and analyzed resonant curve. We have found that variation in radial distance of the satellite increases when time increases. We have also shown the effect of Earth's equatorial ellipticity parameter on different oscillatory amplitudes. We have shown the point R of resonance including angular rate of rotation of the Earth and the rate of change of Earth's equatorial ellipticity parameter with the help of graph.

By defining different perturbations, we studied resonant curve due to angular rate of rotation of the Earth and the rate of change of Earth's equatorial ellipticity parameter and effect of Earth's equatorial ellipticity parameter on resonant curve and oscillatory amplitude. We have shown the undamped and unforced phase portrait. We have shown the phase space by defining Poincare section and by considering the Poincare mapping for the differential equation induced by the solution of that equation. Finally, we have obtained the energy integral in the set of axis rotating with Earth. We have also found equilibrium points of the sum function and motion of the mean longitude.

Acknowledgment:

We are thankful to the Centre for Fundamental Research in Space Dynamics and Celestial Mechanics (CFRSC) for providing all facilities for this research work.

REFERENCES

Bhatnagar, K.B. and Gupta, B. (1977). Resonance in the restricted problem of three bodies with short-periodic perturbations, Proceedings of the Ind. National Sci. Acad., Vol. 43, No. 2, pp. 153–168.

Bhatnagar, K.B. and Kaur, M. (1990). The in-plane motion of geo-synchronous satellite under the gravitational attraction of the sun, the moon and the oblate earth, J. Atrophys. Astr., Vol. 11, No. 1, pp. 1–10.

Breiter, S. (1999). Lunisolar apsidal resonance at low satellite orbits, Celestial Mechanics and Dynamic Astronomy, Vol. 74, No. 4, pp. 253–274.

Brown, E.W. and Shook, C.A. (1993). *Planetary Theory*, Cambridge University Press, Cambridge.

Cai, L., Bu, J., Tang, D., Zhou, M., Yao, R. and Huang, S. (2020). Geosynchronous satellite gf-4 observations of chlorophyll-a distribution details in the Bohai Sea, China. Sensors, Vol. 20, No. 19.

Formiga, J. K. S. and de Moraes, R. V. (2011). 15:1 resonance effects on the orbital motion of artificial satellites, J. Aerosp. Technol. Manag, Vol. 3, No. 3, pp. 251-258.

Frick, R. H. and Garber, T.B. (1962). *Perturbation of Synchronous Satellite*, The RAND Corporation, R-399, NASA.

Garfinkel, B. (1982). On resonance in celestial mechanics (A survey), Celestial Mechanics, Vol. 28, No. 1-2, pp. 275–290.

Gupta, B. and Bhatnagar, K.B. (1992). Resonance in the restricted problem of three bodies, Indian Journal of Pure and Applied Mathematics, Vol. 23, No. 6, pp. 436–476.

Hashimoto, H., Wang, W., Dungan, J. L., Li, S., Michaelis, A. R., Takenaka, H., Higuchi, A., Myneni, R. B. and Nemani, R. R. (2021). New generation geostationary satellite observations support seasonality in greenness of the Amazon evergreen forests, Nature Communications, Vol. 12, No. 1, pp. 1–11.

Kaur, C., Sharma, B. K. and Pandey, L. P. (2018). Resonance in the motion of the geo-centric satel-

lite due to Polynting-Robertson drag, Application and Applied Mathemtics: An International Journal (AAM), Vol. 13, No. 1, pp. 173-189.
Radwan, M. (2002). Resonance caused by the LuniSolar attractions on a satellite of the oblate Earth, Astrophysics and Space Science, Vol. 282, No. 3, pp. 551–562.
Shaw, S. and Holmes, P. (1983). A periodic forced piecewise linear oscillator, Journal of Sound and Vibration, Vol. 90, No. 1, pp. 129-155.
Yadav, S. and Aggarwal, R. (2013). Resonance in a geo-centric satellite due to Earth's equatorial ellipticity, Astrophys Space Sci., Vol. 349, No. 2, pp. 727-743.
Yadav, S., Kumar, V. and Aggarwal, R. (2019). Existance and stability of equilibrium points in the problem of geo-centric satellite including Earth's equatorial ellipticity, Nonlinear Dynamics and System Theory, Vol. 19, No. 4, pp. 537–550.

Appendix

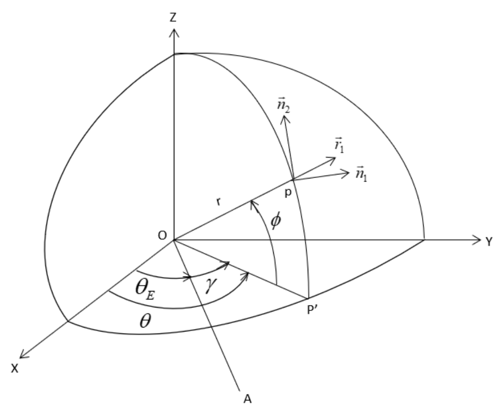

Figure 1. Coordinate System

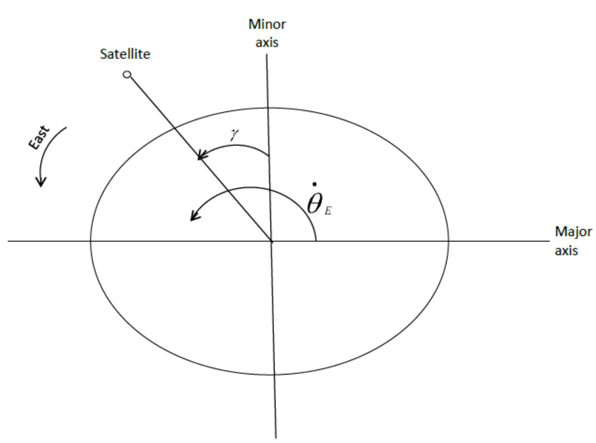

Figure 2. Earth's Equatorial Section

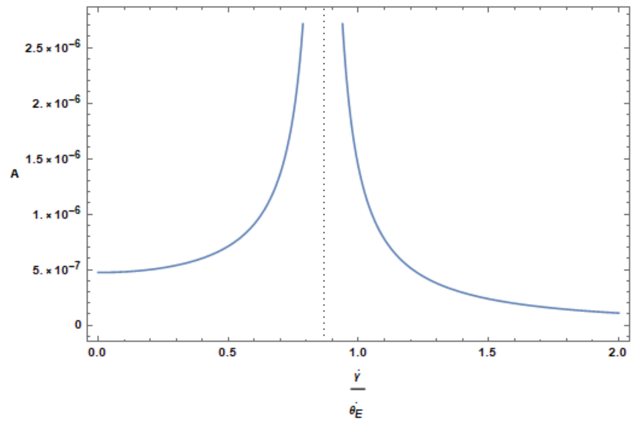

Figure 3. Resonant Curve

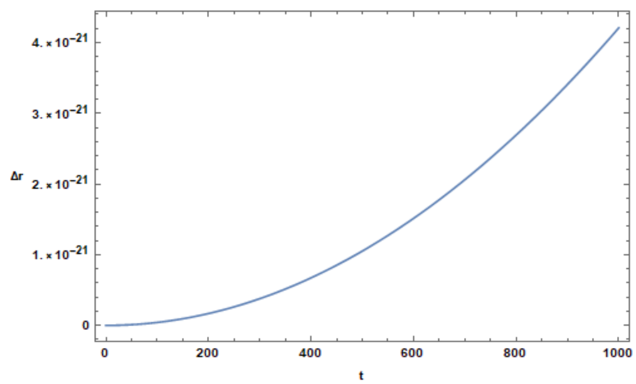

Figure 4. Δr vs time t

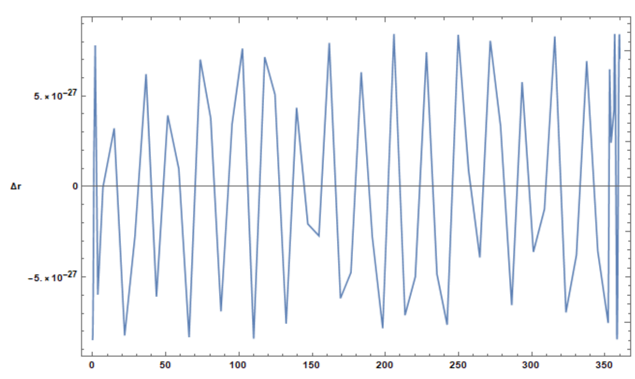

Figure 5. Δr vs Earth's equatorial ellipticity parameter γ

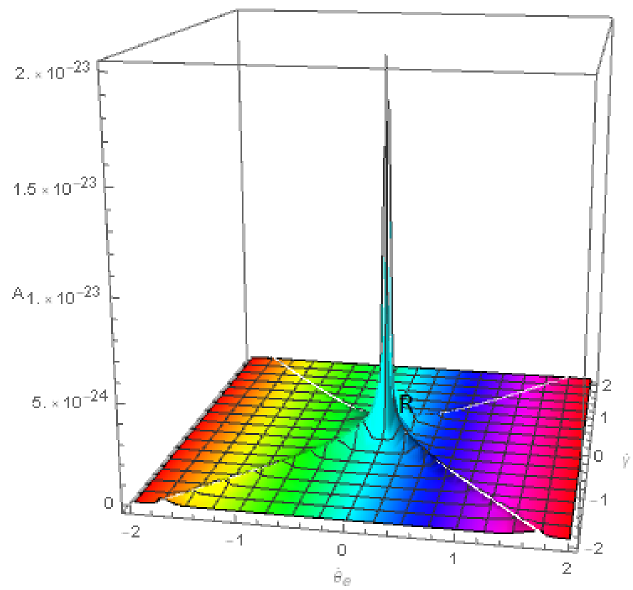

Figure 6. Effect of $\dot{\gamma}$ and $\dot{\theta}_E$ on A

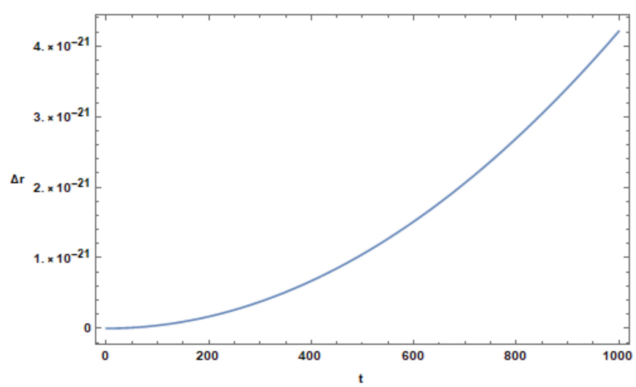

Figure 7. Δr vs time t

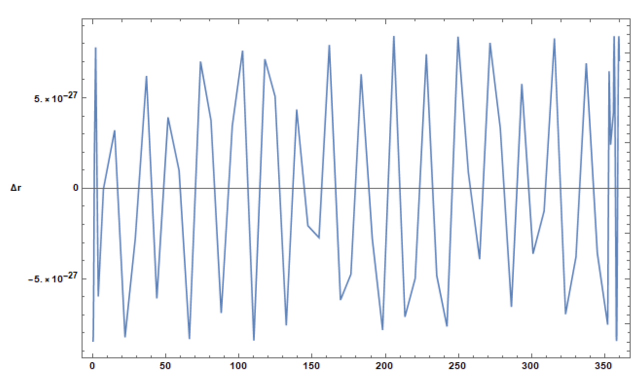

Figure 8. Δr vs Earth's equatorial ellipticity parameter γ

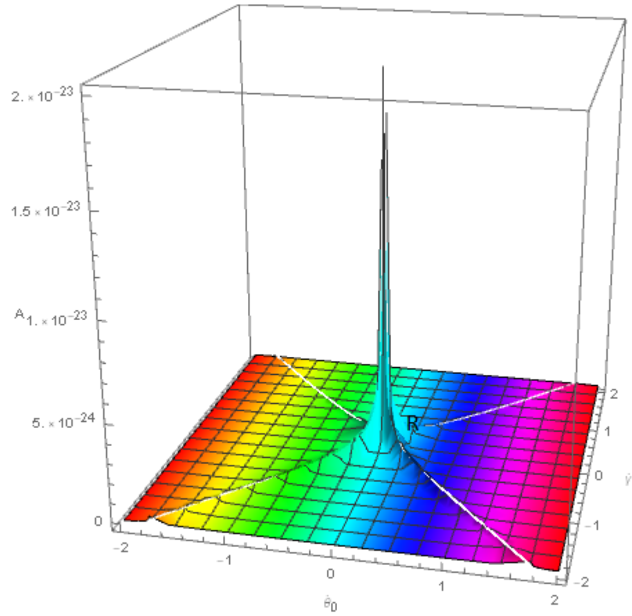

Figure 9. Effect of $\dot{\gamma}$ and $\dot{\theta}_0$ on A

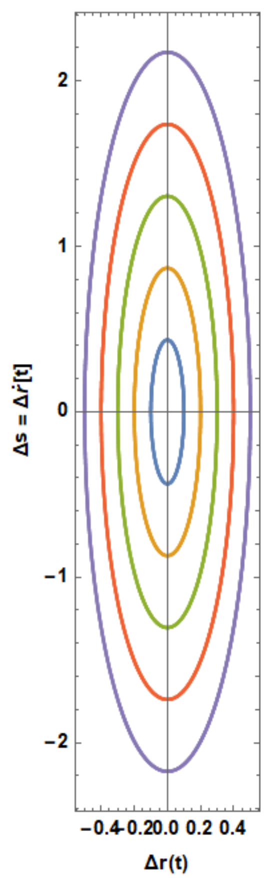

Figure 10. Phase portrait for $K = 0$

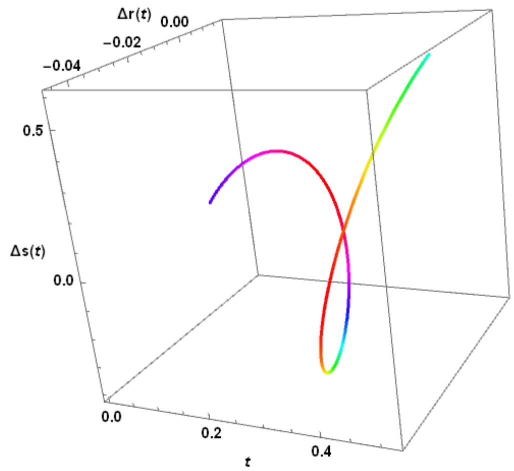

Figure 11. Phase space $(t, \Delta r, \Delta s)$ showing the Poincare section $\sum$ with $\frac{\pi}{\gamma}$ periodicity in t